LNA-mediated anti–miR-155 silencing in low-grade B-cell lymphomas

Yong Zhang,[1] Aldo M. Roccaro,[1] Christopher Rombaoa,[1] Ludmilla Flores,[1] Susanna Obad,[2] Stacey M. Fernandes,[1] Antonio Sacco,[1] Yang Liu,[1] Hai Ngo,[1] Phong Quang,[1] Abdel Kareem Azab,[1] Feda Azab,[1] Patricia Maiso,[1] Michaela Reagan,[1] Jennifer R. Brown,[1] To-Ha Thai,[3] Sakari Kauppinen,[2,4] and Irene M. Ghobrial[1]

[1]Department of Medical Oncology, Dana-Farber Cancer Institute, Harvard Medical School, Boston, MA; [2]Santaris Pharma, Hørsholm, Denmark; [3]Beth Israel Deaconess Medical Center, Harvard Medical School, Boston, MA; and [4]Aalborg University, Copenhagen, Denmark

miR-155 acts as an oncogenic miR in B-cell lymphoproliferative disorders, including Waldenstrom macroglobulinemia (WM) and chronic lymphocytic leukemia, and is therefore a potential target for therapeutic intervention. However, efficient targeting of miRs in tumor cells in vivo remains a significant challenge for the development of miR-155–based therapeutics for the treatment of B-cell malignancies. In the present study, we show that an 8-mer locked nucleic acid anti–miR-155 oligonucleotide targeting the seed region of miR-155 inhibits WM and chronic lymphocytic leukemia cell proliferation in vitro. Moreover, anti–miR-155 delivered systemically showed uptake in the BM CD19$^+$ cells of WM-engrafted mice, resulting in the up-regulation of several miR-155 target mRNAs in these cells, and decreased tumor growth significantly in vivo. We also found miR-155 levels to be elevated in stromal cells from WM patients compared with control samples. Interestingly, stromal cells from miR-155–knockout mice led to significant inhibition of WM tumor growth, indicating that miR-155 may also contribute to WM proliferation through BM microenvironmental cells. The results of the present study highlight the therapeutic potential of anti–miR-155–mediated inhibition of miR-155 in the treatment of WM. (*Blood*. 2012; 120(8):1678-1686)

Introduction

miRs are a class of small, noncoding RNAs (18-23 nt) that control gene expression at the posttranscriptional level by repressing translation or by promoting degradation of the target mRNAs.[1-3] miRs play essential roles in many biologic processes, including development of the immune system and immune response.[4,5] Moreover, deregulated expression of specific miRs is associated with a wide variety of diseases, including both solid and hematopoietic malignancies.[6,7]

Waldenström macroglobulinemia (WM) is a low-grade lymphoproliferative disorder characterized by the presence of an IgM monoclonal protein in the blood and monoclonal small lymphocytes and lymphoplasmacytoid cells in the BM.[8] In chronic lymphocytic leukemia (CLL), a combination of predominant resistance to apoptosis and continuing proliferation leads to progressive accumulation of phenotypically mature malignant lymphocytes.[9] Both diseases are incurable, low-grade, non-Hodgkin B-cell lymphomas.

Epigenetics, including DNA methylation, chromatin remodeling, and miR-mediated regulation of gene expression, has been implicated recently in the pathogenesis of B-cell malignancies.[10,11] We and others have demonstrated that primary WM and CLL cells present with increased expression of miR-155.[12,13] Furthermore, overexpression of miR-155 in B cells of transgenic mice leads to polyclonal pre-B cell proliferation, followed by lymphoblastic leukemia/high-grade lymphoma, indicating that miR-155 plays a crucial role in the pathogenesis of B-cell malignancies and is therefore a potential target for therapeutic intervention. However, reports on pharmacologic inhibition of miR-155 in mouse models of B-cell lymphoma have been lacking.

Locked nucleic acid (LNA) is a conformational analog of RNA in which the ribofuranose ring in the sugar-phosphate backbone is locked in an RNA-like, C3′-endo conformation.[14] This results in high binding affinity between single-stranded, LNA-modified anti-miR oligonucleotides and their complementary miR targets. Several studies have reported on the inhibition of miR function using high-affinity 15- to 16-nt LNA-modified DNA phosphorothioate oligonucleotides targeting the 5′ region of the mature miR.[15-21] Furthermore, a recent study described a method for antagonizing miR function using 8-mer LNA oligonucleotides complementary to the miR seed region, which were called "tiny LNAs."[22]

In the present study, we assessed the efficacy of an 8-mer seed-targeting anti–miR-155 in inhibiting miR-155 function in low-grade non-Hodgkin B-cell lymphoma cells in vitro and in a mouse xenograft model of WM in vivo.

Methods

Cells and reagents

Primary WM cells were collected from the BM of WM patients using CD19$^+$ microbead selection (Miltenyi Biotec) with more than 90% purity, as confirmed by flow cytometric analysis with an mAb against human CD19 (BD Biosciences).[13] Similarly, CD19$^+$ cells were isolated from the BM and peripheral blood of 3 healthy donors and used as controls. Approval for these studies was obtained from the Dana-Farber Cancer Institute Institutional Review Board. Informed consent was obtained from all patients and healthy volunteers in accordance with the Declaration of Helsinki protocol. BCWM1, MEC1, and HEK293 cell lines were used in

Submitted February 15, 2012; accepted June 28, 2012. Prepublished online as *Blood* First Edition paper, July 13, 2012; DOI 10.1182/blood-2012-02-410647.

The online version of this article contains a data supplement.

The publication costs of this article were defrayed in part by page charge payment. Therefore, and solely to indicate this fact, this article is hereby marked "advertisement" in accordance with 18 USC section 1734.

this study. BCWM.1 is a previously described WM cell line derived from $CD19^+$-selected BM lymphoplasmacytic cells isolated from a patient with untreated WM,[23] MEC1 is a cell line derived from B-chronic lymphocytic leukemia in prolymphocytoid transformation,[24] and HEK293 is a human embryonic kidney epithelial cell line (CRL-1573; ATCC). The cell lines were cultured as described previously.[13] BCWM1, MEC1, and mCherry-Luc^+-BCWM1 cells were cultured at 37°C in RPMI 1640 medium containing 10% FBS (Sigma-Aldrich), 2mM L-glutamine, 100 U/mL of penicillin, and 100 μg/mL of streptomycin (Invitrogen). mCherry-Luc^+-BCWM1 cells were generated using lentiviral infection and were a gift from Dr Andrew Kung (Dana-Farber Cancer Institute). Human stromal cells negatively selected by $CD19^+$ microbeads from normal healthy donors or WM patients were cultured at 37°C in DMEM containing 20% FBS, 2mM L-glutamine, 100 U/mL of penicillin, and 100 μg/mL of streptomycin. Mice stromal cells were isolated and cultured as a reference.[25] HEK293 cells stably expressing copepod green fluorescent protein (copGFP) control plasmid or stably expressing pre–miR-155 were generated using PMIRH155PA-1 or pCDH-CMV-MCS-EF1-copGFP cDNA Cloning and Expression Vector (System Biosciences) by lentiviral infection and sorting using the GFP marker. HEK293 and mice stromal cells were cultured at 37°C in DMEM containing 20% FBS, 2mM L-glutamine, 100 U/mL of penicillin, and 100 μg/mL of streptomycin.

DNA synthesis and cytotoxicity assay

Cell proliferation rate and cytotoxicity of BCWM1, MEC1, or stromal cells were measured by DNA synthesis using the $[H]^3$ thymidine uptake assay (PerkinElmer) and by MTT (Chemicon International) dye absorbance, respectively, as described previously.[13,26]

GEP

Total RNA from BCWM1 cells treated with anti–miR-155 or LNA scramble control oligonucleotide, respectively, for 48 hours were isolated using the RNeasy kit (QIAGEN) following the manufacturer's instructions and hybridized on an Affymetrix U133A 2.0 array chip. Gene-expression profiling (GEP) data were analyzed using dChip 2010.01 software (http://biosun1.harvard.edu/complab/dchip/). Candidate target mRNAs for miR-155 were identified using the algorithms TargetScan (http://genes.mit.edu/targetscan/), PicTar (http://pictar.bio.nyu.edu/), and RNAhybrid (http://bibiserv.techfak.uni-bielefeld.de/rnahybrid/). All microarray data are available on the Gene Expression Omnibus public database under accession no. GSE39189.

qRT-PCR

Total RNA of cells was isolated with RNeasy kit (QIAGEN). cDNA was synthesized using SuperScript cDNA synthesis kit (Invitrogen) and quantitative RT-PCR (qRT-PCR) reactions were performed using SYBR Master Mix (SA Bioscience) with designated primers relative to 18S expression by StepOnePlus Real-Time PCR System (Applied Biosystems) in triplicate. TaqMan microRNA Assay kits (Applied Biosystem) were used for quantifying hsa-miR-155 levels relative to RNU6B expression.

Luciferase assays

The oligonucleotides comprising the wild-type or mutated miR-155 target sequences were synthesized by Integrated DNA Technologies, and annealed to be cloned into pMiRGLO vector (Promega) for luciferase reporter assays. The miR-155 target sequences within the 3′-untranslated regions (3′-UTRs) of each target mRNA were predicted by TargetScan, and the sequences are shown below with the wild-type and mutated miR-155 seed match sites underlined. Each construct was confirmed by sequencing at the Molecular Biology Core Facility of Dana-Farber Cancer Institute.

MAFB wild-type: 5′ AAAUACAAAAAAUCUGCAUUAAA 3′ (position 628-634); *MAFB* mutated: 5′ AAAUACAAAAAAUCUCGUAAUAA 3′; *SH3PXD2A* wild-type: 5′ GGAAAUUUCACACUGGCAUUAAC 3′ (position 5426-5432); *SH3PXD2A* mutated: 5′ GGAAAUUAGUGACUGCGUAAUAC 3′; *SHANK2*-1 wild-type: 5′ GUUAUUGAACAAGCAAGCAUUAU 3′ (position 3148-3154); *SHANK2*-1 mutated: 5′ GUUAUUGAACAAGCAUCGUAAUU 3′; *SHANK2*-2 wild-type: 5′ AUCAUGAGAUGAAUGAGCAUUAC 3′ (position 2190-2196); and *SHANK2*-2 mutated: 5′ AUCAUGAGAUGAAUGUCGUAAUC 3′.

HEK293 cells were seeded into 96-well plates and transfected with the constructs harboring wild-type or mutated 3′-UTR target sequences or empty vector as a control. Luciferase activity was measured using the Dual-Glo Luciferase Assay System (Promega). Renilla luciferase activity was normalized to corresponding firefly luciferase activity and is shown as a relative percentage of the control. Experiments were done in triplicate and repeated 3 times.

In vivo studies

Approval of animal studies was obtained by the Dana-Farber Cancer Institute Institutional Animal Care and Use Committees. Six- to 8-week-old, female SCID or Balb/c mice were obtained from Charles River Laboratories. Anesthesia was performed by IP injections of ketamine (80 mg/kg body weight; Bedford Laboratories)/xylazine (12 mg/kg body weight; Lloyd Laboratories).

Balb/c mice were treated with a single IV tail-vein injection of fluorescein amidite (FAM)–labeled anti–miR-155 (synthesized with a complete phosphorothioate backbone and fully LNA modified[22]) or with saline as a control. Live in vivo confocal imaging was used to detect the distribution of the FAM-labeled anti-miR in the mouse BM 1 or 2 weeks after injection (Zeiss 710). Cells from mouse tissues were analyzed by immunofluorescence (Zeiss 710) and flow cytometry (BD FACSCanto II HTS).

Immediately after tail-vein injection of mCherry-Luc^+-BCWM1 cells (3×10^6/mouse) in SCID mice, the mice (6 mice/group) were treated with a single IV tail-vein injection of 25 mg/kg with either anti–miR-155 or LNA scramble control, followed by weekly maintenance doses of 5 mg/kg of anti–miR-155 or LNA scramble control until the mice were killed. Mice were injected with 75 mg/kg of luciferin (Caliper Life Sciences), followed by whole-body real-time bioluminescence imaging (Xenogen IVIS imaging system; Caliper Life Sciences) performed at days 0, 14, and 19. Mice were killed by inhalation of CO_2. RNA was extracted from $CD19^+$ cells isolated from one mouse femur using $CD19^+$ microbead selection. The other femur and the liver and spleen were fixed in formaldehyde. Tissue sections were stained as described previously[13] using Abs against MAFB (Abcam) or CEBPβ (Abcam).

Statistical analysis

Data were analyzed using unpaired Student *t* tests comparing 2 conditions or a 1-way ANOVA with Bonferroni or Newman-Keuls correction for multiple comparisons. $P < .05$ was considered significant and tests were performed 2-sided. Data are presented as means and error bars in the figures depict SD.

Results

Inhibition of miR-155 decreases WM and CLL proliferation in vitro

We first examined the level of miR-155 in primary WM and CLL primary cells, as well as in IgM-secreting low-grade lymphoma cell lines (BCWM1 and MEC1) by qRT-PCR. Our data showed that miR-155 was significantly higher in these samples compared with normal donor $CD19^+$ cells isolated from healthy subjects (supplemental Figure 1, available on the *Blood* Web site; see the Supplemental Materials link at the top of the online article), suggesting that miR-155 may represent a viable therapeutic target in these diseases. To inhibit miR-155 function in malignant cells,

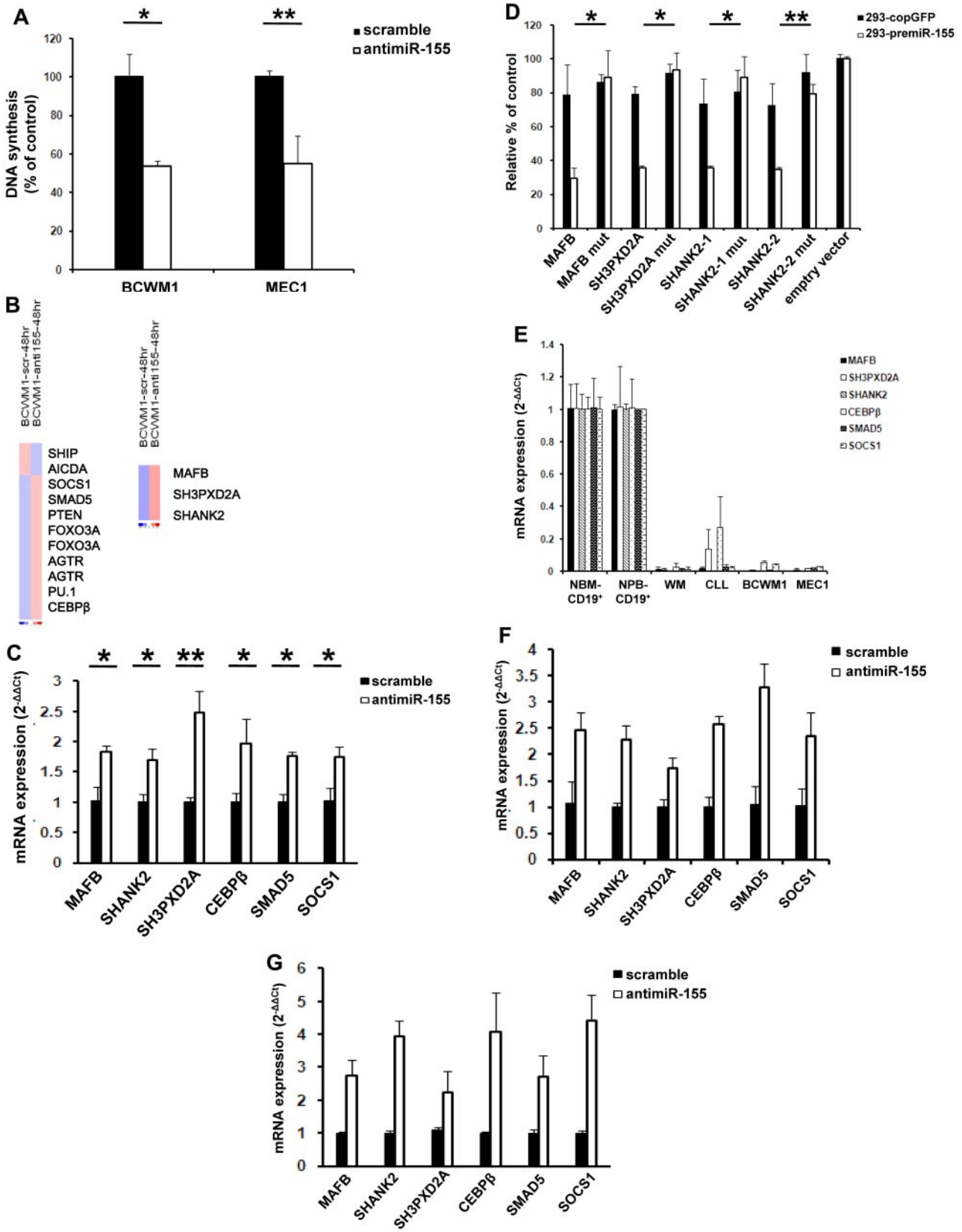

Figure 1. Identification of novel miR-155 target mRNAs in WM. (A) BCWM1 or MEC1 cells were treated with 20μM anti–miR-155 or scramble control for 48 hours. miR-155 inhibition decreases BCWM1 and MEC1 cell proliferation in vitro as evaluated by the $[H]^3$ thymidine uptake assay. Experiments were performed in triplicate and repeated 3 times. Data are shown as means ± SD. $^*P < .05$; $^{**}P < .01$. (B) BCWM1 cells were treated with anti–miR-155 or scramble control for 48 hours. All of the BCWM1 cell samples were cultured and processed in parallel for total RNA extraction and GEP using Affymetrix GeneChip. Validated targets of miR-155 are shown in a heat map on the left and predicted targets of miR-155 are listed on the right. (C) qRT-PCR analysis of selected miR-155 targets in BCWM1 cells treated with anti–miR-155 or scramble control for 48 hours. Experiments were performed in triplicate and repeated 3 times. Data are shown as means ± SD. $^*P < .05$; $^{**}P < .01$. (D) Stable HEK293 cell lines overexpressing pre-miR-155 or empty vector as a control were generated by lentiviral infection. Cells were transiently transfected with the reporter plasmid pmirGLO driving luciferase

we used a fully LNA-modified 8-mer seed-targeting anti–miR-155 (supplemental Figure 2).[22] To assess the uptake of anti–miR-155 into BCWM1 or MEC1 cells, we used a 5′ FAM-labeled anti–miR-155 and added the anti-miR directly to the cell suspension without any transfection reagent. The uptake of FAM-labeled anti–miR-155 into BCWM1 cells was higher than 90% as judged by flow cytometry (data not shown), which indicates efficient delivery of the 8-mer anti-miR into tumor cells. To further examine the functional effect of anti–miR-155 on BCWM1 or MEC1, we measured cell survival and cell proliferation by MTT and $[H]^3$ thymidine uptake assays, respectively. Treatment of BCWM1 or MEC1 cells with 20μM anti–miR-155 or scramble control showed significant reduction in cell proliferation 48 hours after treatment (Figure 1A) with no change in cell cytotoxicity (data not shown), which is consistent with previous findings that miR-155 inhibition regulates cell proliferation but not cell apoptosis.[13]

Identification of novel miR-155 targets in B-cell lymphoma cells

To identify new direct miR-155 targets in B-cell lymphomas, we performed GEP on BCWM.1 cells after treatment with anti–miR-155 or scramble control for 24 or 48 hours. Based on GEP data, we found that several validated miR-155 target mRNAs, such as *CEBPβ*, *SMAD5*, and *SOCS1*, were up-regulated in the BCWM1 cells after treatment with anti–miR-155 compared with cells treated with scramble control (Figure 1B). Moreover, we identified 3 potential new targets of miR-155, *MAFB*, *SHANK2*, and *SH3PXD2A*, as predicted by TargetScan software, which were derepressed 48 hours after anti–miR-155 treatment (Figure 1B). These findings were further validated by qRT-PCR, which confirmed the array data from anti–miR-155–treated BCWM1 cells (Figure 1C).

To functionally validate the miR-155 target mRNA interactions, we generated luciferase 3′-UTR reporters for *MAFB*, *SHANK2*, and *SH3PXD2A*. We used an RNA hybrid to depict the miR-155 target sites in the 3′-UTRs of *MAFB*, *SHANK2*, and *SH3PXD2A*, followed by cloning of the wild-type and mutated target sequences into the pMiRGLO vector (supplemental Figure 3). After transfection of the luciferase reporters into HEK293 cells stably expressing copGFP control plasmid or HEK293 cells stably expressing pre-miR-155 (supplemental Figure 4), dual luciferase activity was measured. A significant repression of the luciferase activity was observed for all 3′-UTR reporters containing a perfect match target site, whereas there was no change in luciferase activity for the reporters harboring mutations in the miR-155 target site sequences, implying that *MAFB*, *SHANK2*, and *SH3PXD2A* are indeed bona fide targets of miR-155 (Figure 1D).

We next used qRT-PCR to determine the mRNA levels of the 6 miR-155 target genes, *SMAD5*, *SOCS1*, *CEBPβ*, *MAFB*, *SHANK2*, and *SH3PXD2A*, in BCWM1 cells from primary WM $CD19^+$ cells, primary CLL cells, normal donor blood $CD19^+$ cells, and BCWM1 and MEC1 cells. We found that all 6 targets were significantly down-regulated in malignant cells in WM or CLL compared with normal control $CD19^+$ cells (Figure 1E). Moreover, treatment of primary WM $CD19^+$ cells or primary CLL cells with 20μM anti–miR-155 for 48 hours showed a significant increase in the mRNA levels of the 6 miR-155 targets compared with scramble control–treated cells as judged by qRT-PCR (Figure 1F-G). In summary, our data indicate that *SMAD5*, *SOCS1*, *CEBPβ*, *MAFB*, *SHANK2*, and *SH3PXD2A* are negatively regulated by miR-155 in WM and CLL.

Delivery of anti–miR-155 into engrafted WM cells in recipient mice

We next investigated whether the anti–miR-155 could be delivered to the BM, where low-grade B-cell malignancies primarily reside. Balb/c mice were dosed with a single IV tail-vein injection of 25 mg/kg of FAM-labeled anti–miR-155 or saline control and examined for distribution after 1 week and 2 weeks by live in vivo confocal imaging. As shown in Figure 2A, the FAM-labeled anti–miR-155 was successfully taken up by cells present in the BM and was detected up to 2 weeks after a single tail-vein injection of the anti–miR-155 compound. We also examined the distribution of FAM-labeled anti–miR-155 in cells of other tissues in the hematopoietic system of the mice, including spleens and femoral BM, by immunofluorescence. Our data showed that the FAM-labeled anti–miR-155 was widely distributed in both the spleen and BM, which show high levels of infiltrated malignant B cells in WM and CLL (Figure 2B). Furthermore, we examined the distribution of FAM-labeled anti–miR-155 in cells from the femur, spleen, and liver using flow cytometric analysis to quantify the ratio of cells that were positive for FAM-labeled anti–miR-155. As shown in Figure 2C, there was a significant shift in the number of FAM^+ cells. These data indicate that the anti–miR-155 could be efficiently delivered and taken up by cells of the hematopoietic system.

We also investigated whether the anti–miR-155 compound could be effectively delivered into WM cells in vivo. To this end, 7 SCID mice per group were engrafted with 3×10^6 mCherry-Luc^+-BCWM1 cells, followed by a single IV tail-vein injection of 25 mg/kg of FAM-labeled anti–miR-155 or saline. Two weeks after injection, mouse femoral BM and spleens were collected for immunofluorescence imaging and, as shown in Figure 2D, our results indicate that FAM-labeled anti–miR-155 could be taken up by engrafted WM cells in the BM and spleens of recipient mice.

Inhibition of miR-155 decreases tumor growth in a xenograft mouse model of WM

To assess the antitumor activity of anti–miR-155 in vivo, we used a xenograft mouse model of WM. Six SCID mice per group were engrafted with 3×10^6 mCherry-Luc^+-BCWM1 cells, after which time mice were injected with a loading dose of 25 mg/kg of anti–miR-155 or scramble control, followed by weekly maintenance doses of 5 mg/kg of each respective compound until the mice were killed. Tumor burden was monitored using bioluminescent imaging at days 0, 14, and 19 after injection (Figure 3A). Image analysis showed that there was a significant reduction in tumor burden at days 14 and 19 in the anti–miR-155–treated mice compared with mice treated with the scramble control (Figure 3B).

Figure 1. (continued) expression with a target gene fragment containing the predicted miR-155 binding site or a mutated binding site as a control. Relative luciferase activity was decreased in miR-155–overexpressing HEK293 cells transfected with plasmids harboring miR-155 target sequences compared with plasmids harboring mutated target sequences. Experiments were performed in triplicate and repeated 3 times. Data are shown as means ± SD. *$P < .05$; **$P < .01$. (E) mRNA levels of miR-155 target genes were detected by qRT-PCR from normal donor blood $CD19^+$ cells, BCWM1 and MEC1 cells, primary WM $CD19^+$ cells, and primary CLL cells. Experiments were performed in triplicate and repeated 3 times. Data are shown as means ± SD. (F) mRNA levels of miR-155 target genes were detected by qRT-PCR from primary WM $CD19^+$ cells treated with 20μM anti–miR-155 or scramble control for 48 hours. Experiments were performed in triplicate and repeated 3 times. Data are shown as means ± SD. (G) mRNA levels of miR-155 target genes were detected by qRT-PCR from primary CLL cells treated with 20μM anti–miR-155 or scramble control for 48 hours. Experiments were performed in triplicate and repeated 3 times. Data are shown as means ± SD.

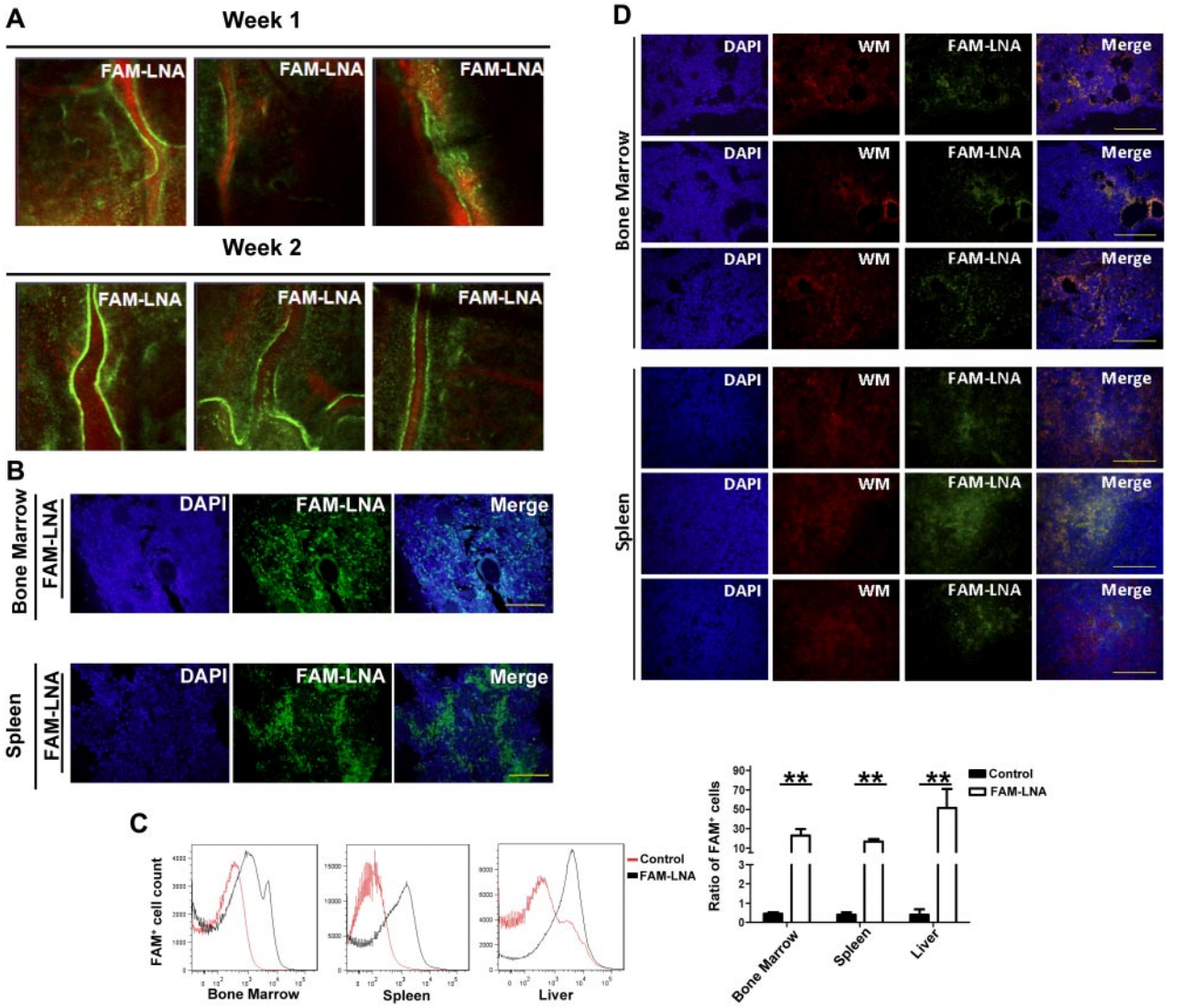

Figure 2. Distribution of FAM-labeled anti–miR-155 in mice. Balb/c mice were dosed with a single tail-vein injection of 25 mg/kg of FAM-labeled anti–miR-155 or saline. (A) Distribution of FAM-labeled anti–miR-155 in cells from mice calvarium BM shown by live in vivo confocal microscopy imaging. Blood vessels are shown by Evans blue staining in red and FAM-labeled anti–miR-155 in green. (B) Distribution of FAM-labeled anti–miR-155 in cells from mice organs shown by immunofluorescent imaging. Cell nuclei are shown by DAPI staining in blue and FAM-labeled anti–miR-155 in green. Scale bar indicates 100 μm. (C) Distribution of FAM-labeled anti–miR-155 in BM, spleen, and liver as measured by flow cytometry. Statistical analysis of flow cytometry results is shown in the lower panel in bar graph. Data are shown as means ± SD. $^{**}P < .01$. (D) Seven SCID mice were dosed with a single tail-vein injection of 25 mg/kg of FAM-labeled anti–miR-155 or saline immediately after injection of mCherry-Luc$^+$-BCWM1 cells. Distribution of FAM-labeled anti–miR-155 in cells from the organs of mice was detected by immunofluorescent imaging and data from 3 representative mice are shown. Cell nuclei are shown by DAPI staining (blue), mCherry-Luc$^+$-BCWM1 cells in red, and FAM-labeled anti–miR-155 in green. Scale bar indicates 100 μm.

No difference in body weight was identified between the 2 groups (data not shown).

We next quantified the mRNA levels of 6 miR-155 targets in the BM WM CD19$^+$ cells by qRT-PCR, which showed that all 6 targets were derepressed after treatment with the anti–miR-155 compared with scramble control (Figure 3C). Moreover, immunostaining confirmed derepression of the MAFB and CEBPβ targets at the protein level in the BM and spleens on treatment with the anti–miR-155 (Figure 3D). These data imply that anti–miR-155–mediated silencing of miR-155 in a xenograft mouse model of WM leads to derepression of direct miR-155 targets in the BM WM CD19$^+$ cells and decreases the tumor growth in recipient mice.

Inhibition of miR-155 decreases WM and CLL proliferation in the context of the BM microenvironment

To examine the effect of anti–miR-155 on tumor progression in the context of the microenvironment, we first quantified the miR-155 levels in BM stromal cells (mesenchymal stem cells) from WM patients compared with normal healthy donors. We found that miR-155 levels in WM stromal cells were higher compared with healthy donor BM stromal cells (Figure 4A). Therefore, we used 20μM anti–miR-155 or scramble control to coculture BCWM1 or MEC1 cells with primary WM BM stromal cells and then assessed cell proliferation by MTT and $[H]^3$ thymidine uptake assays, respectively, after 48 hours. Our results indicate that anti–miR-155 treatment could not only decrease tumor cell proliferation, but also overcame the protective effect induced by coculture of tumor cells with BM stromal cells (Figure 4B). We observed no effect on cell cytotoxicity on stromal cells (data not shown).

Because the BM microenvironment plays a critical role in supporting tumor cell growth, in the present study, we sought to examine the role of miR-155 in tumor proliferation specifically in BM stromal cells. BCWM1 or MEC1 cells were cocultured with BM stromal cells from miR-155–knockout (miR-155$^{-/-}$) mice or

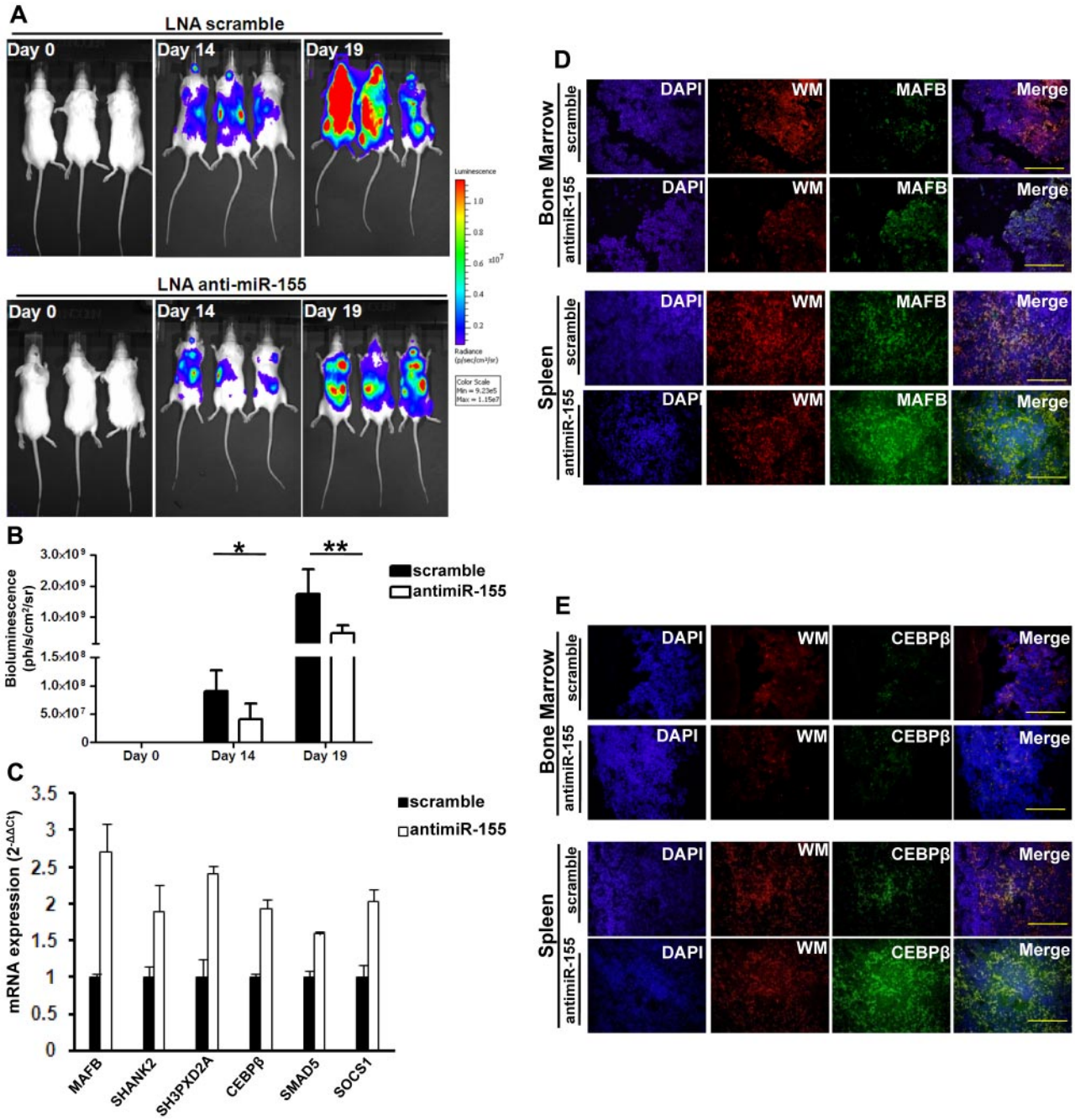

Figure 3. Inhibition of miR-155 decreases tumor growth in a xenograft mouse model of WM. Immediately after injection of mCherry-Luc$^+$-BCWM1 cells, 6 SCID mice per group were injected with a loading dose of 25 mg/kg of anti–miR-155 or scramble control, followed by weekly maintenance doses of 5 mg/kg of anti–miR-155 or scramble control until mice were killed. (A) Bioluminescent imaging of tumor burden from mice injected with mCherry-Luc$^+$-BCWM1 cells at day 0, 14, or 19. (B) Treatment with the anti–miR-155 decreased tumor burden significantly compared with scramble control as evaluated by whole body imaging. Three representative mice from each group are shown. $P = .024$ at day 14; $P = .009$ at day 19 (n = 6 per group). Data are shown as means ± SD. *$P < .05$; **$P < .01$. (C) mRNA levels of miR-155 targets were detected by qRT-PCR in the BM CD19$^+$ cells from mice treated with anti–miR-155 or LNA scramble control. Experiments were performed in triplicate and repeated 3 times. Data are shown as means ± SD. (D-E) Protein levels of the miR-155 target genes MAFB (D) and CEBPβ (E) were detected by immunofluorescent imaging from the femur BM or spleens of mice. Cell nuclei are shown by DAPI staining in blue; mCherry-Luc$^+$-BCWM1 cells in red. MAFB or CEBPβ proteins were detected by immunostaining with anti-MAFB or anti-CEBPβ. Scale bar indicates 100 μm.

wild-type mice as a control. Cell cytotoxicity and cell proliferation were assessed after 48 hours of coculture. The stromal cells from miR-155$^{-/-}$ mice inhibited the proliferation of BCWM1 and MEC1 cells significantly compared with stromal cells from wild-type mice, indicating that miR-155 may also play an important role in the surrounding microenvironmental cells, lending significant support to tumor growth and proliferation (Figure 4C).

To further clarify whether anti–miR-155 can affect both tumor cells and stromal cells, we treated BCWM1 or MEC1 cells with anti–miR-155 or scramble control, followed by coculturing of the treated cells with BM stromal cells from wild-type mice compared with stromal cells from miR-155$^{-/-}$ mice. Cell survival and cell proliferation were assessed by MTT assay and [H]^3 thymidine uptake assays, respectively, after 48 hours of coculture. Our data

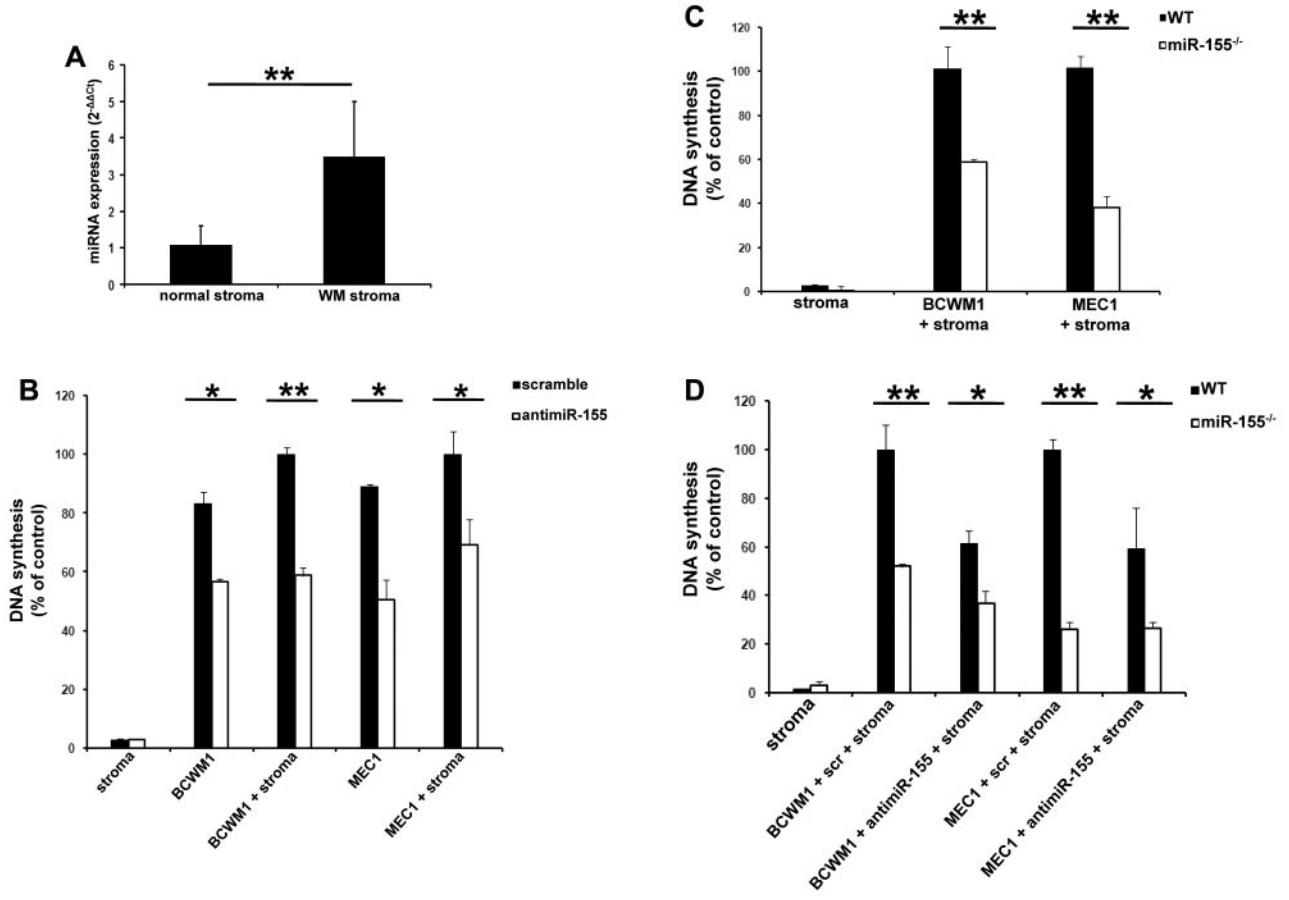

Figure 4. miR-155 inhibition decreases WM and CLL proliferation in the context of the BM milieu. (A) qRT-PCR analysis of miR-155 levels in WM stroma (n = 10) compared with normal stroma (n = 3). Data are shown as means ± SD. $^{**}P < .01$. (B) BCWM1 or MEC1 cells were treated with 20μM anti–miR-155 or scramble control for 48 hours, followed by coculture with stromal cells from WM patients. Cell proliferation was evaluated by $[H]^3$ thymidine uptake assay. Experiments were performed in triplicate and repeated 3 times. Data are shown as means ± SD. $^{*}P < .05$; $^{**}P < .01$. (C) BCWM1 or MEC1 cells were cocultured with stromal cells from wild-type or miR-155$^{-/-}$ mice, and cell proliferation was measured by $[H]^3$ thymidine uptake assay. Experiments were performed in triplicate and repeated 3 times. Data are shown as means ± SD. $^{**}P < .01$. (D) BCWM1 or MEC1 cells were treated with 20μM anti–miR-155 or scramble control for 48 hours, followed by cocultured with stromal cells from wild-type or miR-155$^{-/-}$ mice. Cell proliferation was measured by $[H]^3$ thymidine uptake assay. Experiments were performed in triplicate and repeated 3 times. Data are shown as means ± SD. $^{*}P < .05$; $^{**}P < .01$.

showed that treatment with anti–miR-155 could decrease tumor cell proliferation compared with scramble control when cocultured with wild-type mice stroma, but not significantly on coculturing with miR-155$^{-/-}$ stromal cells, indicating that anti–miR-155 treatment leads to a similar effect on WM as the genetic miR-155 loss-of-function (Figure 4D).

Discussion

miR-155 acts as an onco-miR in many malignancies, especially B-cell lymphoproliferative disorders. Previous studies have shown that miR-155 is a major regulator of oncogenesis in aggressive and low-grade lymphomas.[12,13] However, studies reporting on therapeutic targeting of miR-155 in mouse lymphoma models in vivo have been lacking. In the present study, we used a fully LNA-modified 8-mer anti–miR-155 to inhibit miR-155 function in cultured WM and CLL cells in vitro and in a mouse xenograft model of WM. Our data showed that systemic delivery of the anti–miR-155 resulted in uptake of the compound in the BM, livers, and spleens of mice. The anti–miR-155 compound was also detected in WM cells in the BM and spleens of engrafted recipient mice. Pharmacologic inhibition of miR-155 by systemically delivered anti–miR-155 in a xenograft mouse model of WM resulted in derepression of several direct miR-155 targets in the BM WM CD19$^+$ cells and decreased the tumor growth significantly in recipient mice.

Previous studies have identified several direct targets of miR-155, including *SOCS1*, *FOXO3A*, *AICDA*, *PTEN*, *AGTR1*, *SMAD5*, *SHIP1*, *PU.1*, and *CEBPβ*.[27-36] With the aim of understanding which of the aforementioned targets play a role in the pathogenesis of low-grade B-cell lymphomas, in the present study, we carried out GEP in WM cells and found that 3 known miR-155 targets, *SMAD5*, *SOCS1*, and *CEBPβ*, as well as 3 novel miR-155 targets, *MAFB*, *SHANK2*, and *SH3PXD2A*, were derepressed after anti–miR-155 treatment. MAFB belongs to the MAF family of basic leucine zipper transcription factors.[37] Combined deficiency for the transcription factors MAFB and c-Maf enables self-renewal of differentiated functional macrophages.[38] *Maf* genes, including *MAFB*, are mostly bona fide oncogenes, as highlighted by studies from their initial isolation to their involvement in human cancer.[39] For example, in humans, *Maf* genes are overexpressed in approximately 60% of human angioimmunoblastic T-cell lymphomas[40] and in approximately 50% of multiple myeloma cases, in which they contribute directly to cancer progression.[41-43] However, Maf proteins can be either pro- or antioncogenic, depending on the cell context, and their antioncogenic activity has been linked to their

strong terminal differentiating activity.[44] Therefore, it is tempting to speculate that miR-155 controls cell proliferation through *MAFB* and that MAFB may function as a tumor suppressor in B-cell malignancies, because the expression level of MAFB in lymphoma was found to be lower compared with normal cells. However, further studies are needed to elucidate the role of MAFB, SHANK2, and SH3PXD2A in lymphoma and to shed light on the molecular complexity of the miR-155 pathway in these diseases.

The BM microenvironment, which includes nonmalignant bystander cells and secreted cytokines, plays a crucial role in the pathogenesis of nonHodgkin lymphomas.[45-47] In the present study, we found higher miR-155 levels in the stromal cells of patients with WM compared with those from healthy subjects (Figure 4A). Interestingly, loss of miR-155 in the stroma led to significant inhibition of tumor growth, indicating that miR-155 regulates tumor proliferation not only when it is overexpressed in the malignant cells, but also when it is present in BM microenvironmental cells (Figure 4). The high level of miR-155 in stromal cells and its regulation of tumor growth are intriguing. Recent studies have shown that exosomes could mediate the transfer of mRNAs and miRs as a novel mechanism of genetic exchange and regulation between cells.[48] Future studies are needed to examine the possible exchange of miRs between stromal cells and tumor cells and the mechanisms through which the lack of miR-155 in the stroma regulates tumor growth.

In the present study, we used an 8-mer seed-targeting anti–miR-155 to inhibit miR-155 function in low-grade B-cell lymphomas that harbor high levels of miR-155. Our results indicate that systemically delivered anti–miR-155 antagonizes miR-155 effectively in vivo within the BM microenvironment and other hematopoietic tissues and inhibits tumor growth in a mouse xenograft model of WM in vivo. The results of the present study highlight the potential of the tiny 8-mer anti–miR-155 in therapeutic targeting of miR-155 in hematologic malignancies with aberrant expression of miR-155.

Acknowledgments

This work was supported in part by research grants from the Leukemia & Lymphoma Society, The Kirsch Laboratory for Waldenstrom, and the Heje Fellowship. mCherry-Luc$^+$-BCWM1 cells were a kind gift from Dr Andrew Kung (Dana-Farber Cancer Institute, Harvard Medical School, Boston, MA).

Authorship

Contribution: Y.Z., A.M.R., and I.M.G. designed and performed the research, analyzed the data, and wrote the manuscript; C.R., L.F. S.O., S.M.F., A.S., Y.L., H.N., P.Q., A.K.A., F.A., P.M., and M.R. performed the research; and J.R.B., T.-H.T., and S.K. analyzed the data and edited the manuscript.

Conflict-of-interest disclosure: S.O. and S.K. are employees of Santaris Pharma. I.M.G. is on the advisory board of Millennium-Takeda and Novartis. The remaining authors declare no competing financial interests.

Correspondence: Irene M. Ghobrial, MD, Department of Medical Oncology, Dana-Farber Cancer Institute, 450 Brookline Ave, Boston, MA, 02115; e-mail: irene_ghobrial@dfci.harvard.edu.

References

1. Inui M, Martello G, Piccolo S. MicroRNA control of signal transduction. *Nat Rev Mol Cell Biol.* 2010; 11(4):252-263.
2. Krol J, Loedige I, Filipowicz W. The widespread regulation of microRNA biogenesis, function and decay. *Nat Rev Genet.* 2010;11(9):597-610.
3. Bartel DP. MicroRNAs: target recognition and regulatory functions. *Cell.* 2009;136(2):215-233.
4. Ivey KN, Srivastava D. MicroRNAs as regulators of differentiation and cell fate decisions. *Cell Stem Cell.* 2010;7(1):36-41.
5. Havelange V, Garzon R. MicroRNAs: emerging key regulators of hematopoiesis. *Am J Hematol.* 2010;85(12):935-942.
6. Vasilatou D, Papageorgiou S, Pappa V, Papageorgiou E, Dervenoulas J. The role of microRNAs in normal and malignant hematopoiesis. *Eur J Haematol.* 2010;84(1):1-16.
7. Berdasco M, Esteller M. Aberrant epigenetic landscape in cancer: how cellular identity goes awry. *Dev Cell.* 2010;19(5):698-711.
8. Treon SP, Gertz MA, Dimopoulos M, et al. Update on treatment recommendations from the Third International Workshop on Waldenstrom's macroglobulinemia. *Blood.* 2006;107(9):3442-3446.
9. Chiorazzi N, Rai KR, Ferrarini M. Chronic lymphocytic leukemia. *N Engl J Med.* 2005;352(8): 804-815.
10. Alsayed Y, Ngo H, Runnels J, et al. Mechanisms of regulation of CXCR4/SDF-1 (CXCL12)-dependent migration and homing in multiple myeloma. *Blood.* 2007;109(7):2708-2717.
11. Moreau AS, Jia X, Ngo HT, et al. Protein kinase C inhibitor enzastaurin induces in vitro and in vivo antitumor activity in Waldenstrom macroglobulinemia. *Blood.* 2007;109(11):4964-4972.
12. Wang M, Tan LP, Dijkstra MK, et al. miRNA analysis in B-cell chronic lymphocytic leukaemia: proliferation centres characterized by low miR-150 and high BIC/miR-155 expression. *J Pathol.* 2008; 215(1):13-20.
13. Roccaro AM, Sacco A, Chen C, et al. microRNA expression in the biology, prognosis, and therapy of Waldenstrom macroglobulinemia. *Blood.* 2009; 113(18):4391-4402.
14. Vester B, Wengel J. LNA (locked nucleic acid): high-affinity targeting of complementary RNA and DNA. *Biochemistry.* 2004;43(42):13233-13241.
15. Nicolas FE, Pais H, Schwach F, et al. Experimental identification of microRNA-140 targets by silencing and overexpressing miR-140. *RNA.* 2008; 14(12):2513-2520.
16. Kocerha J, Faghihi MA, Lopez-Toledano MA, et al. MicroRNA-219 modulates NMDA receptor-mediated neurobehavioral dysfunction. *Proc Natl Acad Sci U S A.* 2009;106(9):3507-3512.
17. Castoldi M, Vujic Spasic M, Altamura S, et al. The liver-specific microRNA miR-122 controls systemic iron homeostasis in mice. *J Clin Invest.* 2011;121(4):1386-1396.
18. Eskildsen T, Taipaleenmaki H, Stenvang J, et al. MicroRNA-138 regulates osteogenic differentiation of human stromal (mesenchymal) stem cells in vivo. *Proc Natl Acad Sci U S A.* 2011;108(15): 6139-6144.
19. Montgomery RL, Hullinger TG, Semus HM, et al. Therapeutic inhibition of miR-208a improves cardiac function and survival during heart failure. *Circulation.* 2011;124(14):1537-1547.
20. Elmén J, Lindow M, Schutz S, et al. LNA-mediated microRNA silencing in non-human primates. *Nature.* 2008;452(7189):896-899.
21. Lanford RE, Hildebrandt-Eriksen ES, Petri A, et al. Therapeutic silencing of microRNA-122 in primates with chronic hepatitis C virus infection. *Science.* 2010;327(5962):198-201.
22. Obad S, dos Santos CO, Petri A, et al. Silencing of microRNA families by seed-targeting tiny LNAs. *Nat Genet.* 2011;43(4):371-378.
23. Ditzel Santos D, Ho AW, Tournilhac O, et al. Establishment of BCWM. 1 cell line for Waldenstrom's macroglobulinemia with productive in vivo engraftment in SCID-hu mice. *Exp Hematol.* 2007;35(9):1366-1375.
24. Stacchini A, Aragno M, Vallario A, et al. MEC1 and MEC2: two new cell lines derived from B-chronic lymphocytic leukaemia in prolymphocytoid transformation. *Leuk Res.* 1999;23(2):127-136.
25. Raaijmakers MH, Mukherjee S, Guo S, et al. Bone progenitor dysfunction induces myelodysplasia and secondary leukaemia. *Nature.* 2010; 464(7290):852-857.
26. Leleu X, Jia X, Runnels J, et al. The Akt pathway regulates survival and homing in Waldenstrom macroglobulinemia. *Blood.* 2007;110(13):4417-4426.
27. Kong W, He L, Coppola M, et al. MicroRNA-155 regulates cell survival, growth, and chemosensitivity by targeting FOXO3a in breast cancer. *J Biol Chem.* 2010;285(23):17869-17879.
28. Jiang S, Zhang HW, Lu MH, et al. MicroRNA-155 functions as an OncomiR in breast cancer by targeting the suppressor of cytokine signaling 1 gene. *Cancer Res.* 2010;70(8):3119-3127.
29. Teng G, Hakimpour P, Landgraf P, et al. MicroRNA-155 is a negative regulator of activation-induced cytidine deaminase. *Immunity.* 2008;28(5):621-629.
30. Dorsett Y, McBride KM, Jankovic M, et al. MicroRNA-155 suppresses activation-induced cytidine deaminase-mediated Myc-Igh translocation. *Immunity.* 2008;28(5):630-638.
31. Yamanaka Y, Tagawa H, Takahashi N, et al. Aberrant overexpression of microRNAs activate AKT

signaling via down-regulation of tumor suppressors in natural killer-cell lymphoma/leukemia. *Blood.* 2009;114(15):3265-3275.

32. O'Connell RM, Chaudhuri AA, Rao DS, Baltimore D. Inositol phosphatase SHIP1 is a primary target of miR-155. *Proc Natl Acad Sci U S A.* 2009;106(17):7113-7118.
33. Yin Q, McBride J, Fewell C, et al. MicroRNA-155 is an Epstein-Barr virus-induced gene that modulates Epstein-Barr virus-regulated gene expression pathways. *J Virol.* 2008;82(11):5295-5306.
34. Vigorito E, Perks KL, Abreu-Goodger C, et al. microRNA-155 regulates the generation of immunoglobulin class-switched plasma cells. *Immunity.* 2007;27(6):847-859.
35. Pogribny IP, Starlard-Davenport A, Tryndyak VP, et al. Difference in expression of hepatic microRNAs miR-29c, miR-34a, miR-155, and miR-200b is associated with strain-specific susceptibility to dietary nonalcoholic steatohepatitis in mice. *Lab Invest.* 2010;90(10):1437-1446.
36. Sethupathy P, Borel C, Gagnebin M, et al. Human microRNA-155 on chromosome 21 differentially interacts with its polymorphic target in the AGTR1 3′ untranslated region: a mechanism for functional single-nucleotide polymorphisms related to phenotypes. *Am J Hum Genet.* 2007;81(2):405-413.
37. Kataoka K, Fujiwara KT, Noda M, Nishizawa M. MafB, a new Maf family transcription activator that can associate with Maf and Fos but not with Jun. *Mol Cell Biol.* 1994;14(11):7581-7591.
38. Aziz A, Soucie E, Sarrazin S, Sieweke MH. MafB/c-Maf deficiency enables self-renewal of differentiated functional macrophages. *Science.* 2009;326(5954):867-871.
39. Eychène A, Rocques N, Pouponnot C. A new MAFia in cancer. *Nat Rev Cancer.* 2008;8(9):683-693.
40. Morito N, Yoh K, Fujioka Y, et al. Overexpression of c-Maf contributes to T-cell lymphoma in both mice and human. *Cancer Res.* 2006;66(2):812-819.
41. Hideshima T, Bergsagel PL, Kuehl WM, Anderson KC. Advances in biology of multiple myeloma: clinical applications. *Blood.* 2004;104(3):607-618.
42. Hurt EM, Wiestner A, Rosenwald A, et al. Overexpression of c-maf is a frequent oncogenic event in multiple myeloma that promotes proliferation and pathological interactions with bone marrow stroma. *Cancer Cell.* 2004;5(2):191-199.
43. Boersma-Vreugdenhil GR, Kuipers J, Van Stralen E, et al. The recurrent translocation t(14;20)(q32;q12) in multiple myeloma results in aberrant expression of MAFB: a molecular and genetic analysis of the chromosomal breakpoint. *Br J Haematol.* 2004;126(3):355-363.
44. Pouponnot C, Sii-Felice K, Hmitou I, et al. Cell context reveals a dual role for Maf in oncogenesis. *Oncogene.* 2006;25(9):1299-1310.
45. Steidl C, Connors JM, Gascoyne RD. Molecular pathogenesis of Hodgkin's lymphoma: increasing evidence of the importance of the microenvironment. *J Clin Oncol.* 2011;29(14):1812-1826.
46. Coupland SE. The challenge of the microenvironment in B-cell lymphomas. *Histopathology.* 2011;58(1):69-80.
47. Elsawa SF, Ansell SM. Cytokines in the microenvironment of Waldenstrom's macroglobulinemia. *Clin Lymphoma Myeloma.* 2009;9(1):43-45.
48. Valadi H, Ekstrom K, Bossios A, Sjostrand M, Lee JJ, Lotvall JO. Exosome-mediated transfer of mRNAs and microRNAs is a novel mechanism of genetic exchange between cells. *Nat Cell Biol.* 2007;9(6):654-659.